High-frequency properties of a two-dimensional quantum superlattice in a strong homogeneous electric field

© *L.K. Orlov* [1,2], *T.E. Zedomi* [1], *A.S. Ivina* [1,3], *M.L. Orlov* [3]

[1] Alekseev State Technical University,
603155 Nizhny Novgorod, Russia
[2] Institute of Physics of Microstructures, Russian Academy of Sciences,
603087 Nizhny Novgorod, Russia
[3] Nizhny Novgorod Institute of Management of the President of the Russian Federation,
branch of the Russian Academy of National Economy and Public Administration
of the President of the Russian Federation,
603950 Nizhny Novgorod, Russia

E-mail: orlov@ipm.sci-nnov.ru

The high-frequency conductivity of a two-dimensional quantum superlattice with a rectangular cell and a non-associative electron dispersion law has been studied in the presence of a strong quantizing electric field. The impact of superlattice parameters on the nature of the instability regions of an alternating signal with longitudinal and transverse polarization relative to the applied electric field is considered. It is shown that, in general, the characteristics of the amplified signal are significantly influenced not only by the magnitude and direction of the electric field applied to the superlattice, but also by the parameters of the energy spectrum of electrons in the superlattice. In a constant field directed at an angle to the axes of the superlattice, regions may appear where the instability of an alternating signal with arbitrary polarization is realized only at high frequencies.

Keywords: two-dimensional quantum superlattice, non-associative law of dispersion, anisotropy, constant and alternating electric fields, low-frequency and high-frequency characteristics.

1. Introduction

The use of various materials in the manufacture of low-dimensional quantum heterocompositions of various dimensions makes it relevant to study the influence of the structure of energy zones on their characteristics. The conversion and generation of high-frequency electromagnetic radiation [1–8] are among the most discussed phenomena studied in periodic semiconductor structures. In many cases, however, the reasons for the nonlinear response to the external fields of real systems used in the experiment can be very diverse, including those unrelated to the mechanisms most often used in the literature today to explain the characteristics observed in the experiment. Therefore, the task of diagnosing the band characteristics of electrons in the systems actually studied has not lost its relevance along with a purely practical interest in the effect of Bloch oscillations studied in periodic heterocompositions with narrow zones. This is especially important in conditions of exposure to the structure of strong quantizing fields, which have a noticeable effect on the energy spectrum of charge carriers in it.

The features of the anisotropy of the high-frequency characteristics of a lateral two-dimensional quantum superlattice (2D QSL) with a rectangular supercell in the presence of a strong external constant electric field [9] are analyzed in this paper. The interest in two-dimensional quantum heterocompositions [10–12] is associated with progress in the development of heterotransistors with tunneling electron emission into the nanoscale channel region of the structure [13] and successes in the creation of densely packed ordered arrays of nanocrystalline islands on the surface of heteroepitaxial structures associated with the effect of spatial tunneling [14–16].

Moreover, we studied the impact of the parameters of a lattice cell of a two-dimensional quantum superlattice and the nature of the electron dispersion law formed in the system on the anisotropic, field and frequency characteristics of the nonlinear high-frequency response of the system in the presence of a strong constant electric field within the framework of a single-band model.

2. High-frequency conductivity of a two-dimensional quantum superlattice in the presence of constant and alternating electric fields (general relations)

Further, we study the features of the high-frequency characteristics of the lateral quantum 2D QSL in the presence of homogeneous direct and alternating electric

fields in the plane of the structure, with the law of electron dispersion in a two-dimensional mini-zone more general than the simple harmonic law of dispersion corresponding to the strong coupling approximation and most often used in analysis:

$$\varepsilon(\mathbf{k}) = \varepsilon(k_3) + \varepsilon(\mathbf{k}_\perp) = \varepsilon(k_3)$$
$$+ \Delta_1\{1 - [\Delta_{11}\cos(k_1 d_1) + \Delta_{12}\cos(k_2 d_2)]/(\Delta_{11} + \Delta_{12})\}$$
$$+ \Delta_2\{1 - \delta_0 \cos(k_1 d_1)\cos(k_2 d_2)\}, \qquad (1)$$

where $\varepsilon(\mathbf{k})$ and $\mathbf{k}$ — the energy and wave vector of the electron, k_i — its components, $\Delta_{1(2)}$, Δ_{11}, Δ_{12}, $\delta_0 = \pm 1$ — parameters of the energy zone of a two-dimensional quantum superlattice. Next, we also consider the situation when $d_1 \neq d_2$, $\Delta_{11} \neq \Delta_{12}$ along with the symmetric square lattice $(d_1 = d_2)$, which reflects the specifics of a two-dimensional quantum superlattice with a rectangular cell. The presence of a dissociative ($\sim \Delta_2$) term in (1) results in the formation of additional lateral extremes in the two-dimensional Brillouin zone, the position of which is sensitive both to the choice of direction and to the choice of parameter values, in particular to the change of the sign of the parameter δ_0 in the dispersion law (1). $\varepsilon(k_3) = \varepsilon_0 = \text{const}$ or $\varepsilon(k_3) = \hbar^2 k_3^2 / 2m_3^*$ is chosen as the dependence $\varepsilon(k_3)$. The second situation is typical, for example, for textured polycrystalline matrices with nanoscale grains [17] or for an ordered system of filamentous nanocrystals [18] growing in columns in the vertical direction of the growth plane.

We calculate the high-frequency (HF) characteristics of a two-dimensional quantum superlattice for identifying the features related to the specifics of the law of electron dispersion in k-space using the Boltzmann equation with the collision integral in the approximation of constant relaxation time:

$$\partial f/\partial t + (e/\hbar)E_1(t)\partial f/\partial k_1 + (e/\hbar)E_2(t)\partial f/\partial k_2$$
$$= -(f - f^0)/\tau, \qquad (2)$$

where $f(k, t)$ and $f^0(k)$ — nonequilibrium, perturbed by the field, and equilibrium electron distribution functions. The expression for the current density in this case has the following form

$$\mathbf{j} = (e/4\pi^3\hbar)\int_\Omega f(\mathbf{k})(\partial\varepsilon/\partial\mathbf{k})\partial\mathbf{k}. \qquad (3)$$

The chosen approximation makes it possible to identify the main features of the high-frequency response of the system associated with a specific type of electron dispersion law used in the lower mini-zone, and at the same time take into account the effect of state entanglement in the collision

integral for different directions of a two-dimensional quantum superlattice. We decompose the distribution function into a Fourier series by allocating a time factor $\Phi_{\nu\mu}(t)$ using the periodicity condition:

$$f(k_1, k_2, t) = \sum_{\nu,\mu=-\infty}^{\infty} F_{\nu\mu}\Phi_{\nu\mu}(t)\exp\{i(\nu k_1 d_1 + \mu k_2 d_2)\}. \qquad (4)$$

In the case of the Boltzmann distribution with the law of electron dispersion (1) the expression for $F_{\nu\mu}$ in the integral representation is written as

$$F_{\nu\mu} = F_0 Re \int_0^{2\pi}\partial x_1 \int_0^{2\pi}\partial x_2 \exp(i\nu x_1 + i\mu x_2)$$
$$\times \exp\{Y_{11}\cos(x_1) + Y_{12}\cos(x_2) + Y_2\cos(x_1)\cos(x_2)\}, \qquad (5)$$

where

$$x_{1,2} = k_{1(2)}d_{1(2)}, \quad D_{10} = \Delta_1/\{(\Delta_{11} + \Delta_{12})\}, \quad D_{11} = D_{10}\Delta_{11},$$
$$D_{12} = D_{10}\Delta_{12}, \quad D_{20} = \delta_0\Delta_2, \quad Y_{ij} = D_{ij}/k_B T,$$
$$F_0 = \{(2\pi m_3 k_B T)^{1/2}/16\pi^3\hbar\}\exp\{(\mu_F - \Delta_1 - \Delta_2)/k_B T\}.$$

Here it was assumed that the directions of the vectors $\mathbf{k}_1$ and $\mathbf{k}_2$ coincide with the directions of the main axes of the rectangular lattice $\mathbf{k}_1 \parallel \mathbf{r}_{[100]}$, $\mathbf{k}_2 \parallel \mathbf{r}_{[010]}$. $F_{01} = F_{10}$ follows from (5) at $D_{11} = D_{12}$. In some cases, the evaluation of the values of matrix elements for specific 2D QSL parameters is carried out further.

The function $\Phi_{\nu\mu}(t)$ which is a part of the current density expression, determined by solving the Boltzmann equation for the sum of arbitrary values of constant $\mathbf{E}_0$ and alternating $\mathbf{E}_1$ electric fields $\mathbf{E} = \mathbf{E}_0 + \mathbf{E}_1 \cos\omega t$ with components E_{0i} and E_{1i} $(i = 1, 2)$ at the initial time of switching on the field $t_0 = -\infty$, has the following form (see also Ref. [9,19]):

$$\Phi_{\nu\mu}(t) = \tau^{-1}\left\{J_0(B_{\nu\mu}) + 2\sum_{n=1}^{\infty} J_{2n}(B_{\nu\mu})\cos 2n\omega t\right.$$
$$\left. - 2i\sum_{n=1}^{\infty} J_{2n-1}(B_{\nu\mu})\sin(2n-1)\omega t\right\}$$
$$\times \left\{A_{\nu\mu}^{-1}J_0(B_{\nu\mu}) + 2\sum_{k=1}^{\infty} J_{2k}(B_{\nu\mu})\right.$$
$$\times (A_{\nu\mu}\cos 2k\omega t + 2k\omega\sin 2k\omega t)(A_{\nu\mu}^2 + 4k^2\omega^2)^{-1}$$
$$- 2i\sum_{k=1}^{\infty} J_{2k-1}(B_{\nu\mu})[(2k-1)\omega\cos(2k-1)\omega t$$
$$\left. - A_{\nu\mu}\sin(2k-1)\omega t][A_{\nu\mu}^2 + (2k-1)^2\omega^2]^{-1}\right\}, \qquad (6)$$

where

$$A_{\nu\mu} = \tau^{-1} + i(e/\hbar)(\nu E_{01}d_1 + \mu E_{02}d_2),$$

$$B_{\nu\mu} = (e/\hbar\omega)(\nu E_{11}d_1 + \mu E_{12}d_2),$$

$$E_{01} = E_0\cos\psi_0, \quad E_{11} = E_1\cos\psi_1,$$

$$E_{02} = E_0\sin\psi_0, \quad E_{12} = E_1\sin\psi_1,$$

$\psi_0(\psi_1)$ — angles between the directions of the fields $\mathbf{E}_0(\mathbf{E}_1)$ and the axis (100). Additionally, let's write down expressions for the Stark frequencies of electron oscillations in the superlattice:

$$\Omega_{01} = (ed_1/\hbar)E_{01}, \quad \Omega_{02} = (ed_2/\hbar)E_{02},$$

$$\Omega_{11} = (ed_1/\hbar)E_{11}, \quad \Omega_{12} = (ed_2/\hbar)E_{12}.$$

Matrix elements $\Phi_{\nu\mu}$ at a frequency of ω of an alternating signal, respectively, have the following form:

$$\Phi_{\nu\mu}(\omega) = (-2i\omega/\tau)\Big\{J_0(B_{\nu\mu})J_1(B_{\nu\mu})(A_{\nu\mu}^2 + \omega^2)^{-1}$$

$$+ \sum_{n=1}^{\infty}\Big\{J_{2n}(B_{\nu\mu})\Big\{(2n-1)J_{2n-1}(B_{\nu\mu})[A_{\nu\mu}^2 + (2n-1)^2\omega^2]^{-1}$$

$$+ (2n+1)J_{2n+1}(B_{\nu\mu})[A_{\nu\mu}^2 + (2n+1)^2\omega^2]^{-1}\Big\}$$

$$+ J_{2n-1}(B_{\nu\mu})\Big\{2nJ_{2n}(B_{\nu\mu})[A_{\nu\mu}^2 + 4n^2\omega^2]^{-1}$$

$$- 2(n-1)J_{2n-2}(B_{\nu\mu})[A_{\nu\mu}^2 + 4(n-1)^2\omega^2]^{-1}\Big\}\Big\}\Big\}\cos\omega t$$

$$+ (2i/\tau)A_{\nu\mu}\Big\{J_0(B_{\nu\mu})J_1(B_{\nu\mu})[(A_{\nu\mu}^2 + \omega^2)^{-1} - A_{\nu\mu}^{-2}]$$

$$- \sum_{n=1}^{\infty}\Big\{J_{2n}(B_{\nu\mu})\Big\{J_{2n-1}(B_{\nu\mu})[A_{\nu\mu}^2 + (2n-1)^2\omega^2]^{-1}$$

$$- J_{2n+1}(B_{\nu\mu})[A_{\nu\mu}^2 + (2n+1)^2\omega^2]^{-1}\Big\}$$

$$- J_{2n-1}(B_{\nu\mu})\Big\{J_{2n}(B_{\nu\mu})(A_{\nu\mu}^2 + 4n^2\omega^2)^{-1}$$

$$+ J_{2n-2}(B_{\nu\mu})[A_{\nu\mu}^2 + 4(n-1)^2\omega^2]^{-1}\Big\}\Big\}\Big\}\sin\omega t. \tag{7}$$

The expression (7) is converted to the following form in the approximation of a weak variable signal $\mathbf{E}_1(t)$

$$\Phi_{\nu\mu}(\omega) = (-i/\tau)B_{\nu\mu}\Big\{[\omega(A_{\nu\mu}^2 + \omega^2)^{-1}]\cos\omega t$$

$$- A_{\nu\mu}[(A_{\nu\mu}^2 + \omega^2)^{-1} - 2A_{\nu\mu}^{-2}]\sin\omega t. \tag{8}$$

In the general case, it is not difficult to obtain analytical expressions at the frequency of an alternating signal for the current density components j_1, j_2 directed along the main axes of symmetry. The corresponding expressions for the active (j') and reactive (j'') components of the current components j_1, j_2 along the 2D QSL axes have the following form:

$$j_1' = j_{01}\omega\tau\cos\omega t\Big\{2(\Omega_{11}/\omega)F_{10}D_{11}[1 - \tau^2(\Omega_{01}^2 - \omega^2)]$$

$$\times \Big\{[1 - \tau^2(\Omega_{01}^2 - \omega^2)]^2 + 4\tau^2\Omega_{01}^2\Big\}^{-1}$$

$$+ F_{11}D_{20}\Big\{[(\Omega_{11} + \Omega_{12})/\omega]\Big\{1 - \tau^2[(\Omega_{01} + \Omega_{02})^2 - \omega^2]\Big\}$$

$$\times \Big\{[1 - \tau^2[(\Omega_{01} + \Omega_{02})^2 - \omega^2]]^2 + 4\tau^2(\Omega_{01} + \Omega_{02})^2\Big\}^{-1}$$

$$- [(\Omega_{11} - \Omega_{12})/\omega]\Big\{1 - \tau^2[(\Omega_{01} - \Omega_{02})^2 - \omega^2]\Big\}$$

$$\times \Big\{[1 - \tau^2[(\Omega_{01} - \Omega_{02})^2 - \omega^2]]^2 + 4\tau^2(\Omega_{01} - \Omega_{02})^2\Big\}^{-1}\Big\}\Big\}, \tag{9}$$

$$j_1'' = 2j_{01}\sin\omega t\Big\{2(\Omega_{11}/\omega)F_{10}D_{11}\Big\{[1 + \tau^2(\Omega_{01}^2 + \omega^2)]$$

$$\times \Big\{[1 - \tau^2(\Omega_{01}^2 - \omega^2)]^2 + 4\tau^2\Omega_{01}^2\Big\}^{-1} - 2(1 + \tau^2\Omega_{01}^2)^{-1}\Big\}$$

$$+ F_{11}D_{20}\Big\{[(\Omega_{11} + \Omega_{12})/\omega]\Big\{[1 + \tau^2[(\Omega_{01} + \Omega_{02})^2 + \omega^2]]$$

$$\times \Big\{[1 - \tau^2[(\Omega_{01} + \Omega_{02})^2 - \omega^2]]^2 + 4\tau^2(\Omega_{01} + \Omega_{02})^2\Big\}^{-1}$$

$$- 2[1 + \tau^2(\Omega_{01} + \Omega_{02})^2]^{-1}\Big\} - [(\Omega_{11} - \omega_{12})/\omega]\Big\{[1 + \tau^2$$

$$\times [(\Omega_{01} - \Omega_{02})^2 + \omega^2]]\Big\{[1 - \tau^2[(\Omega_{01} - \Omega_{02})^2 - \omega^2]]^2$$

$$+ 4\tau^2(\Omega_{01} - \Omega_{02})^2\Big\}^{-1} - 2[1 + \tau^2(\Omega_{01} - \Omega_{02})^2]^{-1}\Big\}\Big\}\Big\}, \tag{10}$$

$$j_2' = j_{02}\omega\tau\cos\omega t\Big\{2(\Omega_{12}/\omega)F_{01}D_{12}[1 - \tau^2(\Omega_{02}^2 - \omega^2)]$$

$$\times \Big\{[1 - \tau^2(\Omega_{02}^2 - \omega^2)]^2 + 4\tau^2\Omega_{02}^2\Big\}^{-1}$$

$$+ F_{11}D_{20}\Big\{[(\Omega_{11} + \Omega_{12})/\omega][1 - \tau^2[(\Omega_{01} + \Omega_{02})^2 - \omega^2]]$$

$$\times \Big\{[1 - \tau^2[(\Omega_{01} + \Omega_{02})^2 - \omega^2]]^2 + 4\tau^2(\Omega_{01} + \Omega_{02})^2\Big\}^{-1}$$

$$+ [(\Omega_{11} - \Omega_{12})/\omega][1 - \tau^2[(\Omega_{01} - \Omega_{02})^2 - \omega^2]]$$

$$\times \Big\{[1 - \tau^2[(\Omega_{01} - \Omega_{02})^2 - \omega^2]]^2 + 4\tau^2(\Omega_{01} - \Omega_{02})^2\Big\}^{-1}\Big\}\Big\}, \tag{11}$$

$$j_2'' = 2j_{02}\sin\omega t\Big\{2(\Omega_{12}/\omega)F_{01}D_{12}\Big\{[1+\tau^2(\Omega_{02}^2+\omega^2)]$$

$$\times\Big\{[1-\tau^2(\Omega_{02}^2-\omega^2)]^2+4\tau^2\Omega_{02}^2\Big\}^{-1}-2(1+\tau^2\Omega_{02}^2)^{-1}\Big\}$$

$$+F_{11}D_{20}\Big\{[(\Omega_{11}+\Omega_{12})/\omega]\Big\{[1+\tau^2[(\Omega_{01}+\Omega_{02})^2+\omega^2]]$$

$$\times\Big\{[1-\tau^2[(\Omega_{01}+\Omega_{02})^2-\omega^2]]^2+4\tau^2(\Omega_{01}+\Omega_{02})^2\Big\}^{-1}$$

$$-2[1+\tau^2(\Omega_{01}+\Omega_{02})^2]^{-1}\Big\}+[(\Omega_{11}-\Omega_{12})/\omega]\Big\{[1+\tau^2$$

$$\times[(\Omega_{01}-\Omega_{02})^2+\omega^2]]\Big\{[1-\tau^2[(\Omega_{01}-\Omega_{02})^2-\omega^2]]^2$$

$$+4\tau^2(\Omega^{01}-\Omega_{02})^2\Big\}^{-1}-2/[1+\tau^2(\Omega_{01}-\Omega_{02})^2]^{-1}\Big\}\Big\}\Big\}.$$

(12)

Here

$$j_{01}=j_0/\eta,\quad j_{02}=j_0,\quad j_0=eF_0/2\pi\hbar d_1,\quad \eta=d_2/d_1.$$

Let's express the power absorbed at the frequency of the alternating signal. $P_\omega=(\overline{\mathbf{j'E_1}})=\overline{j_1'E_{11}}+\overline{j_2'E_{12}}$ (here the dash indicates time averaging) through the dimensionless components of the high-frequency conductivity tensor $\sigma_{\alpha\beta}'$ [19,20]:

$$P_\omega/P_0=\{\eta^{-1}\sigma_{11}'\cos^2\psi_1+(1+\eta)\sigma_{12}'\cos\psi_1\sin\psi_1$$
$$+\eta^2\sigma_{22}'\sin^2\psi_1\},$$

(13)

where $P_0=j_0E_{cr}$, $E_{cr}=\hbar/ed_1\tau$:

$$\sigma_{11}'=2F_{10}D_{11}[1-\tau^2(\Omega_{01}^2-\omega^2)]\Big\{[1-\tau^2(\Omega_{01}^2-\omega^2)]^2$$

$$+4\tau^2\Omega_{01}^2\Big\}^{-1}+F_{11}D_{20}\Big\{\Big\{1-\tau^2[(\Omega_{01}+\Omega_{02})^2-\omega^2]\Big\}$$

$$\times\Big\{[1-\tau^2[(\Omega_{01}+\Omega_{02})^2-\omega^2]]^2+4\tau^2(\Omega_{01}+\Omega_{02})^2\Big\}^{-1}$$

$$-\Big\{1-\tau^2[(\Omega_{01}-\Omega_{02})^2-\omega^2]\Big\}\Big\{[1-\tau^2[(\Omega_{01}-\Omega_{02})^2-\omega^2]]^2$$

$$+4\tau^2(\Omega_{01}-\Omega_{02})^2\Big\}^{-1}\Big\},$$

(14)

$$\sigma_{12}'=\sigma_{21}'=F_{11}D_{20}\Big\{\Big\{1-\tau^2[(\Omega_{01}+\Omega_{02})^2-\omega^2]\Big\}$$

$$\times\Big\{[1-\tau^2[(\Omega_{01}+\Omega_{02})^2-\omega^2]]^2+4\tau^2(\Omega_{01}+\Omega_{02})^2\Big\}^{-1}$$

$$+\Big\{1-\tau^2[(\Omega_{01}-\Omega_{02})^2-\omega^2]\Big\}\Big\{[1-\tau^2[(\Omega_{01}-\Omega_{02})^2-\omega^2]]^2$$

$$+4\tau^2(\Omega_{01}-\Omega_{02})^2\Big\}^{-1}\Big\},$$

(15)

$$\sigma_{22}'=2F_{01}D_{12}[1-\tau^2(\Omega_{02}^2-\omega^2)]\Big\{[1-\tau^2(\Omega_{02}^2-\omega^2)]^2$$

$$+4\tau^2\Omega_{02}^2\Big\}^{-1}+F_{11}D_{20}\Big\{\Big\{1-\tau^2[(\Omega_{01}+\Omega_{02})^2-\omega^2]\Big\}$$

$$\times\Big\{[1-\tau^2[(\Omega_{01}+\Omega_{02})^2-\omega^2]]^2+4\tau^2(\Omega_{01}+\Omega_{02})^2\Big\}^{-1}$$

$$-\Big\{1-\tau^2[(\Omega_{01}-\Omega_{02})^2-\omega^2]\Big\}$$

$$\times\Big\{[1-\tau^2[(\Omega_{01}-\Omega_{02})^2-\omega^2]]^2+4\tau^2(\Omega_{01}-\Omega_{02})^2\Big\}^{-1}\Big\}.$$

(16)

3. High-frequency conductivity and instability regions of an alternating signal in a two-dimensional superlattices with symmetric and asymmetric potential

The current-voltage curve analysis performed in Ref. [9] for a rectangular lattice ($\eta\neq1$; $D_{11}\neq D_{12}$), in general, except the directions along the main axes of symmetry ($\mathbf{r}_{[100]}$, $\mathbf{r}_{[010]}$), showed a mismatch of the field directions (angle ψ_0) and the current flowing through the structure (angle φ_0). Inclusion in the law of variance (1) the nonadditive term ($D_{20}\neq0$) affects the form of the current-voltage curve of the superlattice (SL), resulting in a shift of the maximum current-voltage curve to the region of higher or lower field values relative to the critical field of nonlinearity E_{cr}, and in strong fields to the possibility of occurrence on the current characteristic, in some cases, an additional second maximum. At the same time, changing the sign of the parameter δ_0 to (1) did result in the formation of any additional features on the structure that could be used to diagnose the inversion of the central valley in the two-dimensional mini-zone of the superlattice.

Next, we will calculate the characteristics of the high-frequency conductivity of 2D QSL. The features of generating signals of different polarization relative to the direction of the constant electric field applied to the SL, depending on the parameters Δ_{11}, Δ_{12} in the electron dispersion law, will be analyzed (1) and the ratios of the periods of the system along the main axes of the lattice $\eta=d_2/d_1$. First of all, let's consider situations when the polarization of the alternating electric field either coincides with the direction of the applied constant electric field ($\psi_1=\psi_0$), or the fields E_0 and E_1 are mutually perpendicular ($\psi_1=\psi_0+\pi/2$). In the simplest case, when the direction of the applied electric field coincides with the main axis $\mathbf{r}_{[100]}$ of high symmetry, i.e. at $\psi_0=0$, the expression (13) for the power absorbed

at a frequency ω has a simple form:

$$P_\omega/P_0 = \eta^{-1}\sigma_{11}'(E_1/E_{cr})^2 = (2/\eta)F_{10}D_{11}$$

$$\times [1 - \tau^2(\Omega_{01}^2 - \omega^2)]\{[1\tau^2(\Omega_{01}^2 - \omega^2)]^2 + 4\tau^2\Omega_{01}^2\}^{-1} \tag{17}$$

at $\psi_1 = \psi_0$ and

$$P_\omega/P_0 = \eta^2\sigma_{22}'(E_1/E_{cr})^2 = 2\eta^2 F_{01}D_{12}/(1 + \tau^2\omega^2) \tag{18}$$

at $\psi_1 = \pi/2$. Thus, a weak alternating signal is amplified in the frequency range $\omega^2 < \Omega_{01}^2 - \tau^{-2}$ with longitudinal polarization of radiation along the direction of the electric field similar to the situation with one-dimensional superlattice; the signal attenuates at all frequencies with transverse polarization. The dependence of the final result on the presence of a dissociative term in the law of dispersion is manifested through the ratio of the values $F_{10}D_{11}$ and $F_{01}D_{12}$. The conductivities responsible for the absorption and amplification of the signal power, namely, at the frequency $\omega\tau = 2$ with $E_0 = 3E_{cr}$, $\psi_0 = 0$ and the values of the parameters of the law of dispersion: $\Delta_1 = 5$ MeV, $\Delta_2 = 1$ MeV, $k_B T = 7$ MeV, $\delta_0 = 1$, $\Delta_{11} = 1$, $\Delta_{12} = 3(30)$, $\eta = 1$ and the corresponding values of the matrix elements: $F_{10} = 4.60613$ (1.54909), $F_{01} = 11.3697$ (14.5723), $F_{11} = 2.57457$ (1.84242), equal to -0.885795 (-0.038439) for $\psi_1 = \psi_0$ and 17.0546 (28.2044) for $\psi_1 = \psi_0 + \pi/2$. Gain (absorption) of HF signal with longitudinal (transverse) polarization decreases (increases) with an increase of potential asymmetry, i.e. with an increase of the ratio Δ_{12}/Δ_{11}.

A similar situation is realized if the direction of the applied electric field coincides with the axis $\mathbf{r}_{[010]}$, i.e., at $\psi_0 = \pi/2$. The corresponding expression (13) for the power absorbed at a frequency of ω in this case has the following form:

$$P_\omega/P_0 = \eta^2\sigma_{22}'(E_1/E_{cr})^2 = 2\eta^2 F_{01}D_{12}$$

$$\times [1 - \tau^2(\Omega_{02}^2 - \omega^2)]\{[1 - \tau^2(\Omega_{02}^2 - \omega^2)]^2 + 4\tau^2\Omega_{02}^2\}^{-1} \tag{19}$$

at $\psi_1 = \psi_0$ and

$$P_\omega/P_0 = \eta^{-1}\sigma_{11}'(E_1/E_{cr})^2 = (2/\eta)F_{10}D_{11}/(1 + \tau^2\omega^2) \tag{20}$$

at $\psi_1 = 0$. As in the previous case, we have an amplification of a weak high-frequency signal in the frequency range $\omega^2 < \Omega_{02}^2 - \tau^{-2}$ for longitudinal polarization of an alternating field, the signal attenuation takes place at all frequencies for transverse polarization. However, the conductivity of the system at the frequency $\omega\tau = 2$ at $\psi_0 = \pi/2$ is respectively equal to -6.55947 (-10.8479) for $\psi_1 = \psi_0$ and 2.30307 (0.0999413) for $\psi_1 = 0$. We obtain the values -3.06119 (7.9591) for the longitudinal (transverse) polarization $\psi_1 = \psi_0(\psi_0 + \pi/2)$ for the conductivity of the square superlattice as in the previous case. Thus, the signal gain with polarization longitudinal along the direction of the constant electric field depends both on the direction of the

latter and decreases (increases) in the first (second) case. We obtain $F_{10}D_{11} = F_{01}D_{12} = 7.9591$ in the absence of potential asymmetry, i.e., at $\Delta_{12} = \Delta_{11}$. We obtain averaged values equal to -3.06119 with longitudinal polarization of radiation ($\psi_1 = \psi_0$) and 7.9591 with transverse polarization for the conductivity of a structure with a symmetric superlattice potential for the power gain (absorption) factor $(P_\omega/P_0)/(E_1/E_{cr})^2$, respectively ($\psi_1 = \psi_0 + \pi/2$).

Let's consider a more complicated case when the direction of the electric field does not coincide with the direction of any axis of high symmetry ($\psi_0 \neq 0$, $\pi/2$) of a square ($d_1 = d_2$) two-dimensional superlattice. Accordingly, solid lines with symbols for several values of superlattice parameters in Figures 1, 2 represent the boundaries of the signal instability regions ($P_\omega = 0$) on the plane ($\omega\tau$, $\Omega_0\tau$). We will assume that the electric field is directed at an angle $9°$ ($\psi_0 = \pi/20$), and we will select the following values for the polarization of the alternating field E_1: $\psi_1 = \psi_0$ and $\psi_1 = \psi_0 + \pi/2$. We take into account the contribution of the dissociative term in the electron dispersion law for calculations ($\Delta_2 \neq 0$). Additionally, we will assume the type of potential to be symmetric ($\Delta_{11} = \Delta_{12}$) or asymmetric ($\Delta_{11} \neq \Delta_{12}$).

The dependences shown on Figure 1 are characterized by the presence of areas of negative conductivity, which cause an increase in the HF signal. The calculation shows that the amplification of an alternating signal with transverse constant field polarization in a certain range of values of a constant electric field can be manifested only at high frequencies (curves *2* in Figure 1, *b, d*) despite the fact that the region of negative differential conductivity (NDC) in a square 2D QSL with a symmetrical potential for the characteristic values of the system parameters and the angles of inclination of the field E_0 is always manifested on the superlattice current-voltage curve in fields greater than critical ($E_0 > E_{cr}$) (curves *1* in Figure 1, *a, c*). That is, the presence of an incident section of the current-voltage curve for fields $E_0 \gg E_{cr}$ in the general case of an arbitrary direction of the acting fields in the system does not guarantee the manifestation of negative conductivity of the alternating signal concurrently at low and high frequencies.

The difference of the values of the field components along the axes $x_{1,2}$ is the reason for the change of the type and nature of the instability regions for an HF signal with longitudinal and transverse polarization. There is no gain of the transverse component of the HF current when the field E_0 is directed along the specified axes. The formation of levels in the electron spectrum in strong fields of the Stark ladder (and associated Bloch oscillations, which cause the appearance of an incident section on the current-voltage curve of the system) results in the instability of the component of the alternating signal polarized along the axis x_1 at the first stage at $E_0 \cos\psi_0 > E_{cr}^{(1)}(j_{01})$ and only afterwards along the axis x_2 with slightly larger values of the field $E_0 \sin\psi_0 > E_{cr}^{(2)}(j_{02})$. Absorption at low frequencies usually exceeds the gain efficiency, therefore, the absorption of a
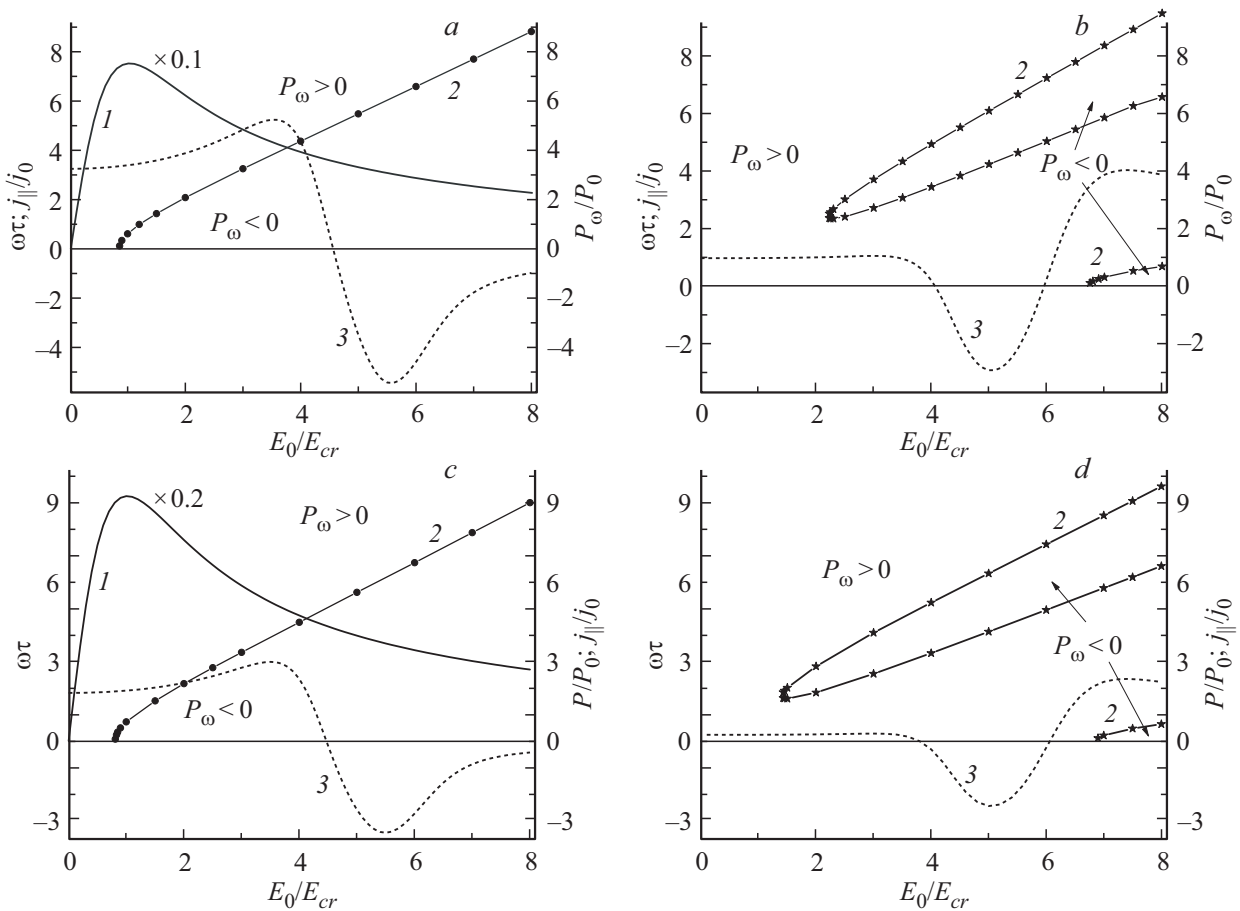
Figure 1. View of the superlattice current-voltage curve (curves *1*) and the instability region of the high-frequency signal for the field direction $\psi_0 = \pi/20$ (solid lines connected by symbols — curves *2*) for $\psi_1 = \psi_0$ *(a, c)*, $\psi_1 = \psi_0 + \pi/2$ *(b, d)*; absorbed signal power P_ω at frequency $\omega\tau = 5$ (dashed lines) — curves *3* depending on the magnitude of the applied electric field E_0. The following was accepted for other parameters: $d_1 = d_2$; $\Delta_{11} = \Delta_{12} = 1$, $\Delta_1 = \Delta_2 = 5$ meV, $k_B T = 7$ meV, $\delta_0 = 1$ *(a, b)*, -1 *(c, d)*.

low-frequency signal is observed in the range of fields E_0 satisfying the above conditions. The gain has maximum values at high frequencies near the instability boundary and the opposite situation is observed, i.e., the signal gain at high frequency will dominate the absorption. Thus, the nature of the instability regions observed in Figure 1, *b, d* is a sheer consequence of the combined manifestation of the above-mentioned mechanisms of amplification and absorption of the components of the field E_1 along the axes x_1 and x_2 of the superlattice.

The case of a square 2D QSL with an asymmetric potential ($\Delta_{11} < \Delta_{12}$) In Figure 2 is considered in contrast to the previous situation. From the type of curves shown in Figure 2, *a* (curves *1*) and corresponding to the boundaries of the amplified signal, the instability regions of the alternating signal have a more complex appearance, even in the case of longitudinal polarization ($\psi_1 = \psi_0$) of high-frequency radiation. Namely, the instability regions undergo narrowing and a shift towards higher values of the constant electric field E_0 in case of the longitudinal polarization of the alternating signal. Thus, there can be no amplification of the alternating signal not only with the

transverse (curves *2* in Figure 2, *b, d*), but with longitudinal polarization (curves *2* in Figure 2, *a, c*) at low frequencies in fields exceeding the critical field E_{cr} despite the drop of current characteristics with an increase of the field E_0 (curves *1* in Figure 2).

At the same time, the amplification of the alternating field E_1 is still possible at high frequencies. A similar situation is observed for a structure with a symmetric potential only for radiation with transverse polarization (see Figure 1). It should be noted that the considered situation is very similar to a one-dimensional superlattice where the electron transitions between the levels of the Stark stairs of two adjacent mini-zones play a significant role [5,21,22]. In this case, the effect of negative dynamic conductivity also arises due to the competition of two different mechanisms of generation and absorption of a high-frequency signal in the system. Thus, there is a range of fields $E_0 > E_{cr}$ in a two-dimensional superlattice, when the field E_0 deviates from the direction of the axes of high symmetry, where, the instability at low frequencies causing the appearance of electric domains, will not occur despite the presence of an incident section on a stationary
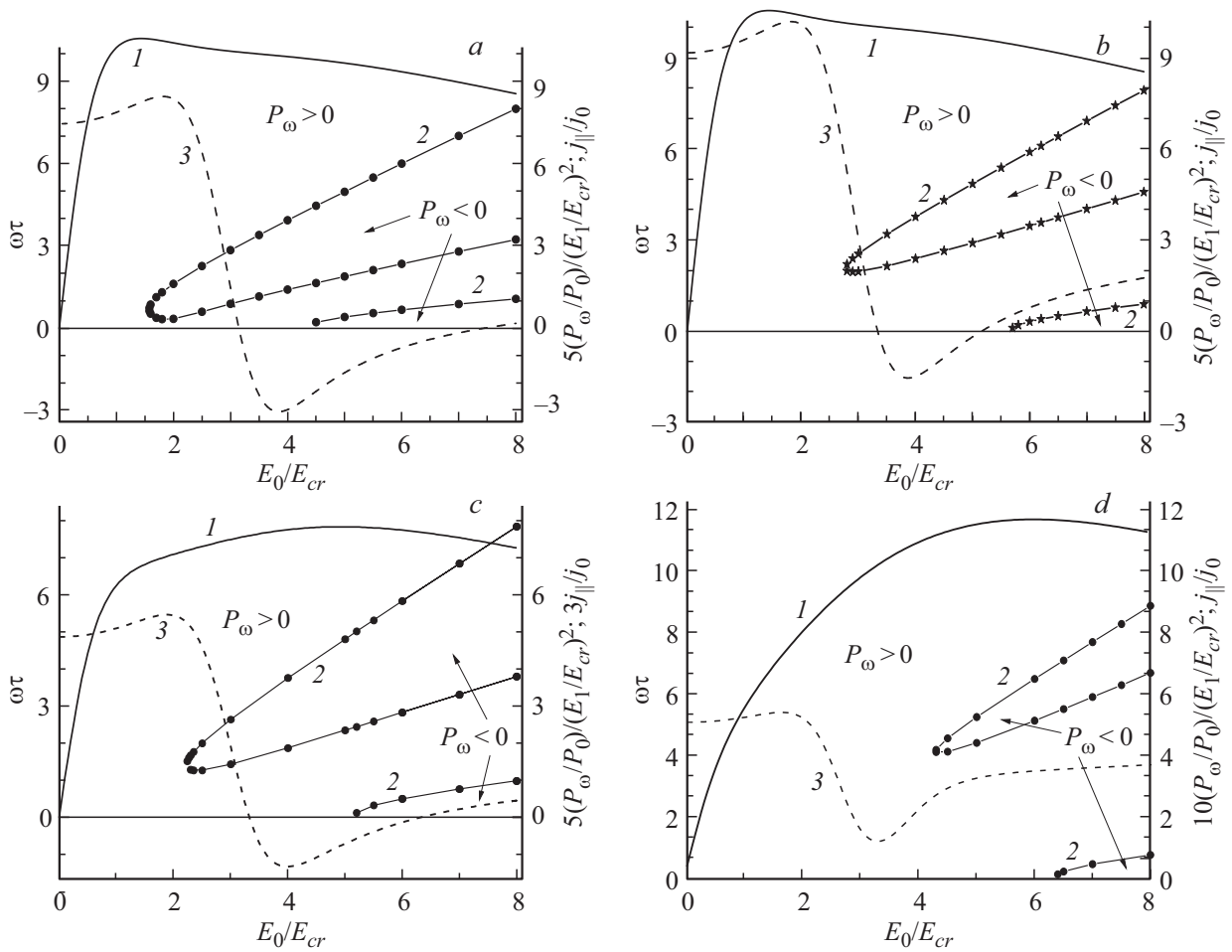
Figure 2. Boundaries of high-frequency signal instability regions (solid lines *2* with symbols), field dependences of the current component (curves *1*) and the power of the absorbed signal P_ω (curves *3* — dashed lines) at a given frequency $\omega\tau = 3$ at constant angle of inclination of the field E_0 ($\psi_0 = \pi/20$) and two polarization angles ψ_1 of the alternating field E_1: $\psi_1 = \psi_0$ (*a, c, d*); $\psi_1 = \psi_0 + \pi/2$ (*b*). The following was assumed for the remaining parameters of the two-dimensional square superlattice: $d_2 = d_1$, $\Delta_1 = 5\,\mathrm{MeV}$; $\Delta_2 = 1\,\mathrm{MeV}$; $\Delta_{11} = 1$, $\Delta_{12} = 3$ (*a, b, c*), 30 (*d*); $\delta_0 = 1$ (*a, b, d*), -1 (*c*); $k_\mathrm{B}T = 7\,\mathrm{meV}$.

current-voltage curve system. In this case, the gain region at high frequencies is realized for variable fields with both polarizations, and the features are a consequence of the competition of nonlinearity mechanisms associated with transitions between states of Stark ladders along the directions of the main axes of superlattice arising under the action of field components $E_{01(2)}$.

A comparison of the curves in Figures 1 and 2, having opposite sign values of the parameters δ_0, but the same values of the other parameters in the law of electron dispersion, shows that the replacement of the parameter $\delta_0 = 1(a)$ by $\delta_0 = -1(c)$ in the dispersion law, which causes the inversion of the central valley in the lower mini-zone of the superlattice, without changing the qualitative appearance of the curves describing the high-frequency characteristics of the system, results in their insignificant quantitative changes. In particular, a shift of the gain regions to the range of higher electric fields and a slight narrowing of them mainly from the low frequencies is

observed. The low-frequency superlattice current-voltage curve (curves *1*) is subject to slightly greater changes, where a shift of the incident section of the current-voltage curve and the associated amplification region of low-frequency signals into the range of higher fields is observed. At the same time, the amplification region at high frequencies experiences a smaller shift, as can be seen from the comparison of the curves in Figure 2, *a, c*, making it possible to dynamically amplify high-frequency radiation even in fields corresponding to the increasing portion of the current-voltage curve.

The impact of the value of the parameter Δ_{12} on the position of the amplification regions of the alternating signal is more significant. This, in particular, can be seen when comparing the curves *2* in Figure 2, *a* and *d*. With a change of the potential within the lattice cell of the superlattice, resulting, in particular, in an increase of the parameter Δ_{12} in the electron dispersion law, the amplification regions of the high-frequency signal E_1 shift noticeably more strongly

towards higher fields. At the same time, the effect of negative dynamic conductivity on the increasing section of the current-voltage curve persists. The analysis of the curves in Figure 2 also allows making a conclusion that it is possible to expect a rotation of the plane of polarization of the alternating field towards the direction of the applied constant field for an alternating signal E_1 with arbitrary polarization relative to the direction of the applied electric field E_0. The effect is attributable to significant differences in the values of high-frequency conductivity for the components of the field E_1 with longitudinal and transverse polarization.

4. Comparison of low-frequency and high-frequency characteristics of electrons in 2D QSL with different values of energy spectrum parameters

Let's consider the nature of instability regions in a quantum superlattice with a rectangular $(d_1 \neq d_2)$ cell. The corresponding field dependences of the direct current components in the directions along $j_\parallel$ and across j_{tr} of the direction of the applied electric field E_0 at a fixed angle ψ_0 were analyzed in Ref. [9]. The nature of the incident area on the superlattice current-voltage curve can noticeably narrow at certain angles of inclination of the field, due to a change in the contribution to $j_\parallel$ of the current components j_1 and j_2. At the same time, there may be an increase rather than a decrease of the current characteristic $j_\parallel$ in strong fields at certain angles of inclination of the field with an increase of the value of the field E_0. We will also consider a more general situation in this section (see Figures 3, 4) corresponding to the deviation of the shape of the lattice cell of the superlattice from the square shape $(d_1 \neq d_2)$. The calculation of the absorbed high-frequency power makes it possible to compare the low-frequency and high-frequency characteristics of the system and trace the relationship between the position of the negative differential conductivity on the current-voltage curve and the position of the amplification regions of the high-frequency signal on the plane $(\omega\tau, E_0/E_{cr})$ depending on the ratio of the lattice periods. In particular, it follows from Figure 3 that even in the case of dominance of the associative term in the electron dispersion law $(\Delta_1 \gg \Delta_2)$, a change in the parameter η, i.e., a deviation of the shape of the superstructure cell from the square shape, affects both superlattice current-voltage curve (Figure 3, a), and in the form of frequency characteristics of an alternating signal polarized both along (Figure 3, b) a constant electric field $(\psi_1 = \psi_0)$ and in the transverse direction (Figure 3, c).

An increase of the role of the dissociative term in the electron dispersion law, i.e., deviation from a purely harmonic dependence (going beyond the approximation of a strong bond), results in noticeable changes in both the type of the superlattice current-voltage curve (Figure 4, a) and the behavior of the gain factor of a high-frequency signal.
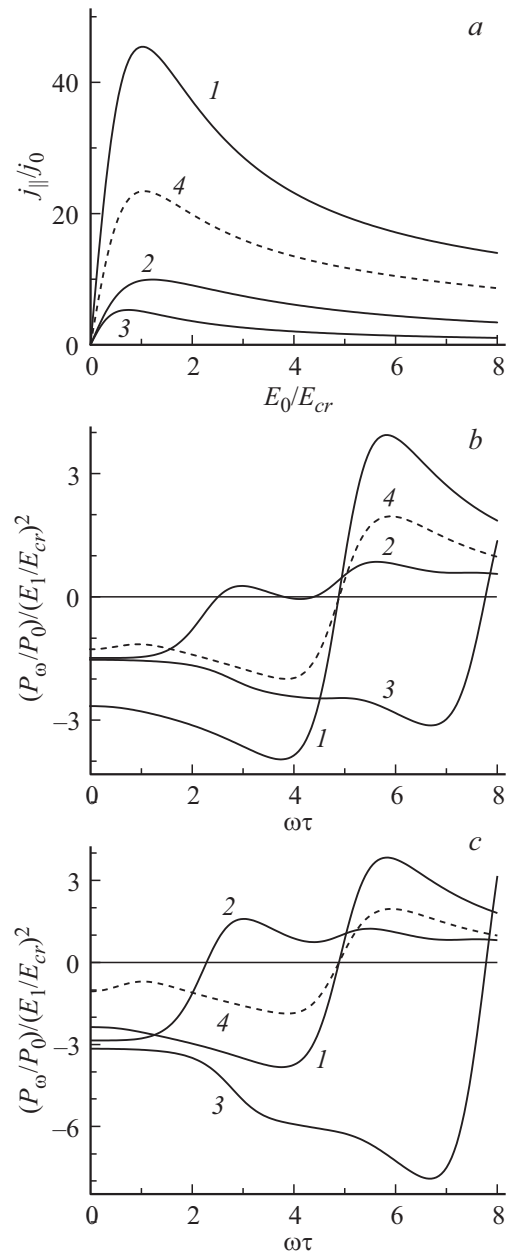
Figure 3. Current (a) and frequency (b, c) characteristics of absorbed microwave power in case of polarization ψ_1 of an alternating field: b — $\psi_1 = \psi_0$, c — $\psi_0 + \pi/2$ and the relation of constant lattices: curve 1 — $d_2/d_1 = 1/2$, 2 —$3/1$, 3 — $10/1$, 4 — $1/1$. The values were selected for the other parameters: $E_0 = 5E_{cr}$, $\psi_0 = \pi/20$, $\Delta_1 = 5$ meV, $\Delta_2 = 1$ meV; $\Delta_{11} = \Delta_{12} = 1$, $\delta_0 = 1$, $k_B T = 7$ meV.

In the considered case (the curves in Figures 3, a and 4, a), the presence of a dissociative term in the electron dispersion law results only in quantitative changes, practically without changing the qualitative appearance of the current-voltage curve superlattice.

With an increase of the parameter Δ_2, both for the longitudinal and transverse polarization of the alternating field, an increase of the gain factor and an expansion
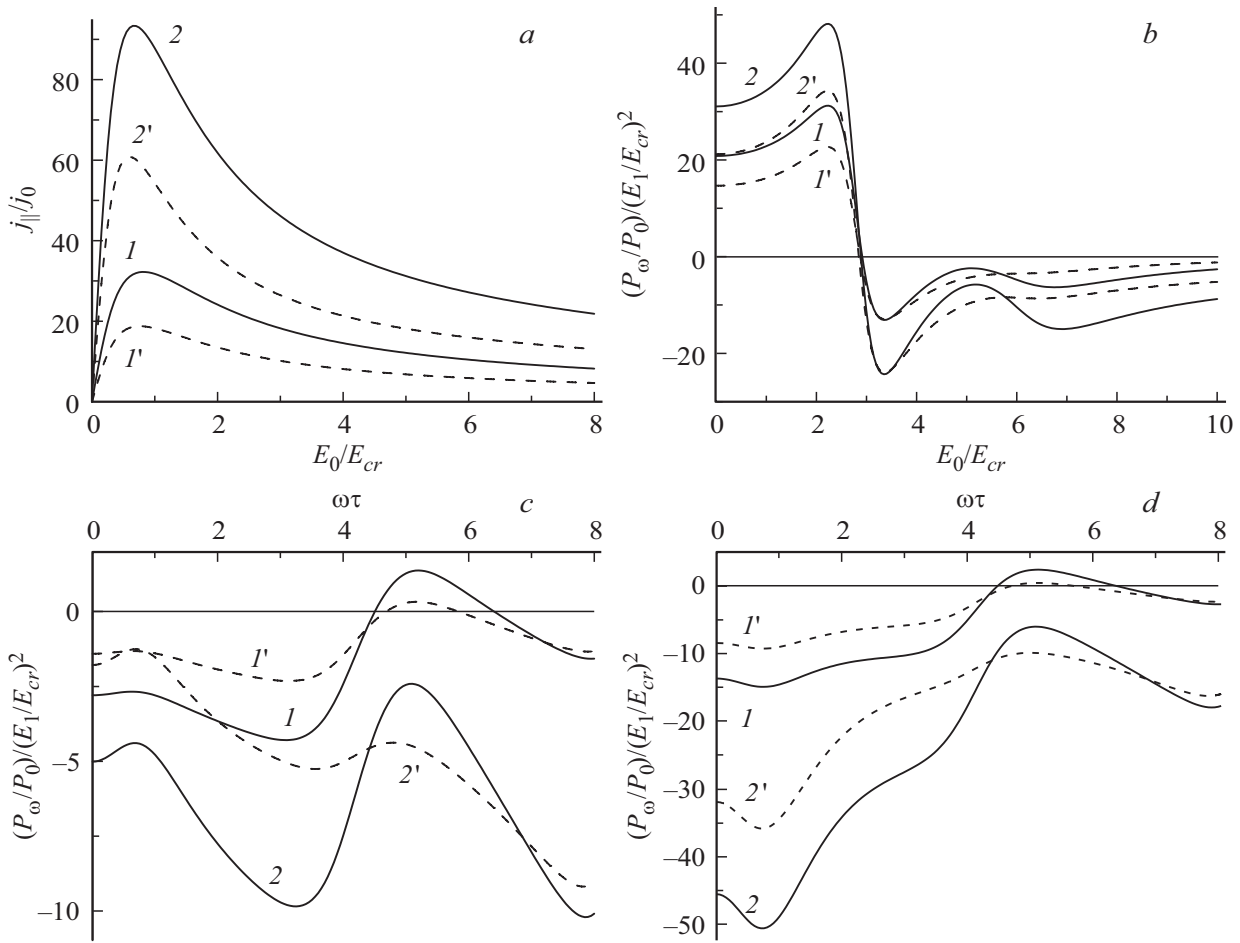
Figure 4. Field (a, b) at $\omega\tau = 5$ and frequency (c, d) at $E_0/E_{cr} = 5$ dependencies a) of current-voltage curve of a two-dimensional quantum superlattices and $b-d$) absorbed power P_ω with polarization ψ_1 of the alternating field: $\psi_1 = \psi_0$ (curves $1, 1'$) and $\psi_1 = \psi_0 + \pi/2$ (curves $2, 2'$) and parameter values Δ_2 (meV) = a, b) 5 (curves $1, 1', 2, 2'$); c, d) 5 (curves $1, 1'$), 10 (curves $2, 2'$); $\delta_0 = 1$ (solid curves), -1 (dashed curves). The following values of remaining parameters of the two-dimensional superlattice were used: $d_2/d_1 = 2.7$, $\psi_0 = \pi/10$, $\Delta_1 = 5$ meV, $\Delta_{11} = \Delta_{12} = 1$, $k_B T = 7$ meV.

of the amplification regions of high-frequency radiation is observed, which follows from the type of curves shown in the frequency dependences of Figure 4, c, d at the fixed value of the applied constant field, and from the field dependencies shown in Figure 4, b. At the same time, as we already indicated in the previous section, additional HF signal absorption regions may appear in the system at intermediate frequencies associated with the oscillatory behavior of the absorbed power in case of a change of the signal frequency (Figure 4, c, d) or the magnitude of a constant electric field (Figure 4, b). The structure of the instability regions changes slightly with a change of the polarization of the alternating electric field, but strongly depends on the parameters of the dispersion law, which, for example, is clearly shown in Figure 5.

Let us consider in more detail the effect of the inversion of the central valley on the high-frequency properties of 2D QSL due to the change in the sign of the parameter δ_0 in the dispersion law. In this case, we will consider 2D QSL with a cell elongated in the transverse direction ($\eta = 2.7$)

and assume the following: $\Delta_2 = \Delta_1$ and $\Delta_{11} = \Delta_{12}$. The qualitative form of the low-frequency characteristic of the superlattice at a fixed field direction (Figure 4, a) practically does not change with a change of the parameters of the electron dispersion law. However, the latter have a rather noticeable effect on the type of high-frequency characteristics, in particular on the structure of the amplification regions of the high-frequency signal. Figure 5 shows the corresponding curves on the plane ($\omega\tau, E_0/E_{cr}$). A comparison of the curves in Figure 5 shows the nature of the change of the amplification regions of high-frequency radiation with a change of its polarization, on the one hand, and with a change of the parameter δ_0 in the dispersion law, on the other hand. We observe the appearance of an additional gain region in the high frequency range (Figure 5, a, c) at $\delta_0 > 0$, areas where the signal is absorbed appear in the amplification area at $\delta_0 < 0$ (Figure 5, b, d). The amplification of radiation with transverse polarization turns out to be more effective at low frequencies according to the curves in Figure 4, 5, while the opposite situation is
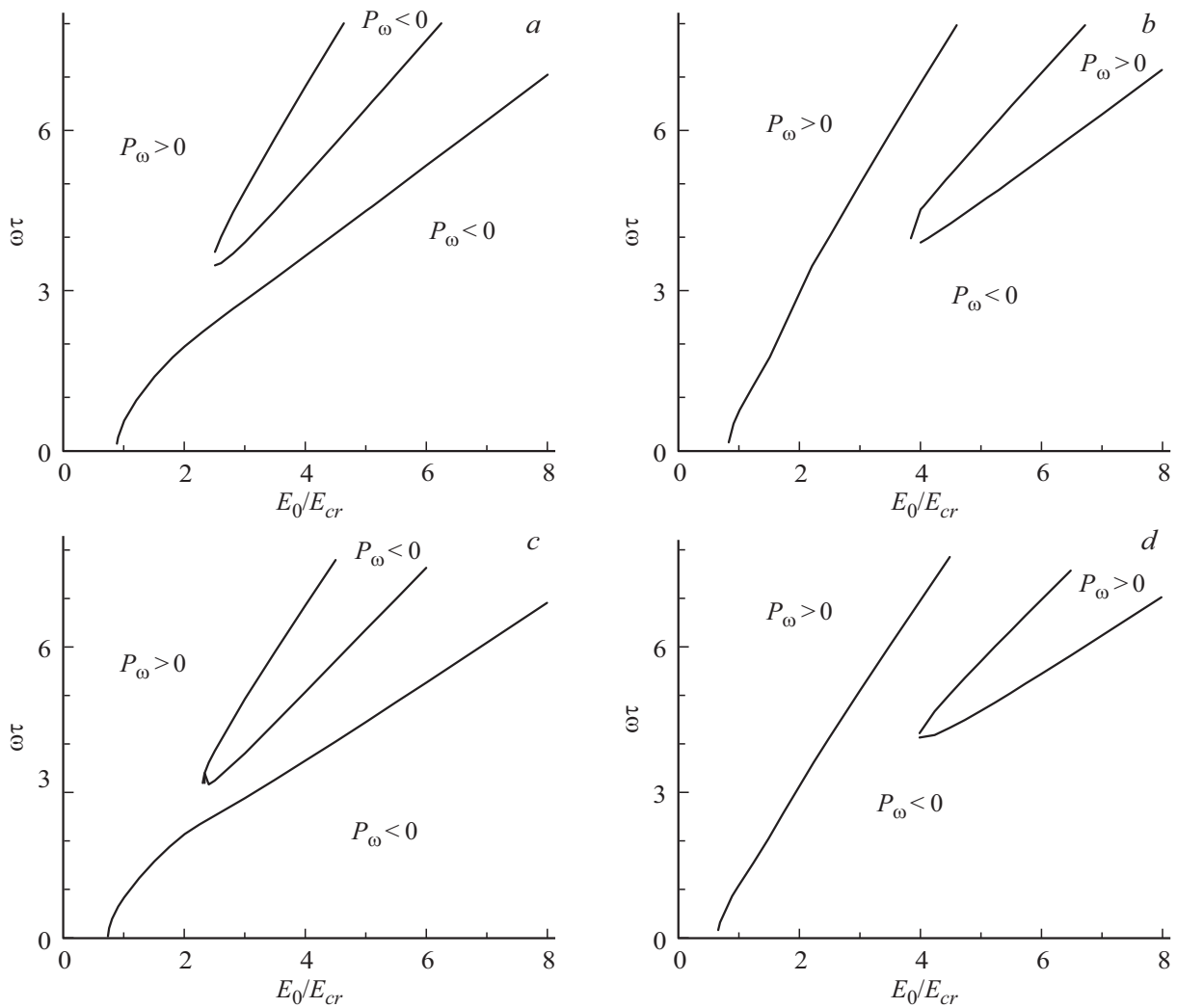
Figure 5. Boundaries of instability regions ($P_\omega < 0$) of a high-frequency signal in the plane ($\omega\tau$, E_0/E_{cr}) for $\psi_1 = \psi_0$ (a, b); $\psi_0 + \pi/2$ (c, d) for the parameter values of a two-dimensional superlattice: $d_2/d_1 = 2.7$, $\psi_0 = \pi/10$, $\Delta_1 = \Delta_2 = 5$ meV, $\Delta_{11} = \Delta_{12} = 1$, $\delta_0 = 1$ (a, c); -1 (b, d); $k_BT = 7$ meV.

observed at high frequencies. Moreover, the amplification of a high-frequency signal, regardless of its polarization, turns out to be significantly higher in a system with a dissociative dispersion law ($\Delta_2 \gg \Delta_1$) than in a system with a purely associative dispersion law.

5. Conclusion

The features of high-frequency conductivity are discussed for the first time in this paper for a two-dimensional quantum superlattice in the presence of a strong quantizing electric field directed at an arbitrary angle relative to the main axes of the structure. Structures with a supercell of rectangular shape and a non-associative electron dispersion law corresponding to exiting the strong bond approximation are considered. The main attention is paid to the effect of the deviation of the shape of the superlattice cell from the ideal square shape, as well as the parameters of the electron

dispersion law on the frequency and field dependences of the high-frequency response of the system to radiation with longitudinal and transverse polarization relative to the applied constant electric field. The impact of these system parameters on the nature of the formation of areas of instability of an alternating signal is studied and they were compared with the corresponding type of superlattice current-voltage curve. It is shown for the considered system that there is a range of parameters for which there are value ranges where the instability of the HF signal will manifest itself only at high frequencies, while there is no amplification of the alternating field at low frequencies. In general, the characteristics of the amplified signal depend not only on the magnitude and direction of the electric field, frequency and polarization of the alternating signal, but also on the nature of the electron energy spectrum formed in a narrow mini-zone of the superlattice.

Conflict of interest

The authors declare that they have no conflict of interest.

References

[1] A. Wacker. Phys. Reports, **357**, 1 (2002).

[2] Yu.A. Romanov, Yu.Yu. Romanov. FTT, **46**, 162 (2004). (in Russian).

[3] A.A. Andronov, I.M. Nefedov, A.V. Sosnin. FTP, **37**, 378 (2003). (in Russian).

[4] D.G. Paveliev, N.V. Demarina, Yu.I. Koshurinov, A.P. Vasiliev, E.S. Semenova, A.E. Zhukov, V.M. Ustinov. FTP, **38**, 1141 (2004). (in Russian).

[5] A.A. Andronov, E.P. Dodin, D.I. Zinchenko, Y.N. Nozdrin, M.A. Ladugin, A.A. Marmalyuk, A.A. Padalitsa, V.A. Belyakov, I.V. Ladenkov, A.G. Fefelov. Pis'ma ZhETF **102**, 235 (2015). (in Russian).

[6] H. Eisele, L. Li, E.H. Linfield. Appl. Phys. Lett., **112**, 172103 (2018).

[7] D.G. Pavelyev, A.P. Vasilev, V.A. Kozlov, E.S. Obolenskaya, S.V. Obolensky, V.M. Ustinov. IEEE Trans. TGz Sci. Technol., **8**, 231 (2018).

[8] M.F. Pereira, A. Apostolakis. Nanomaterials, **11**, 1287 (2021).

[9] M.L. Orlov, L.K. Orlov. FTP, **55**, 241 (2021). (in Russian).

[10] Yu.A. Romanov, E.V. Demidov. FTP, **31**, 308 (1997). (in Russian).

[11] I.A. Dmitriev, R.A. Suris. FTP, **36**, 1449 (2002). (in Russian).

[12] D.V. Zavyalov, V.I. Konchenkov, S.V. Kryuchkov. FTP, **53**, 1527 (2019). (in Russian).

[13] J. Lee, R. Lee, S. Kim, K. Lee, H.-M. Kim, S. Kim, M. Kim, S. Kim, J.-Ho Lee, B.-G. Park. Solid State Electron., **164**, 107701 (2020).

[14] X. Huang, Ch. Liu, P. Zhou. 2D Mater. Applications, **51**, 1 (2022).

[15] S.A. Rudin, Zh.V. Smagina, V.A. Zinovyev, P.L. Novikov, A.V. Nenashev, E.E. Rodyakina, A.V. Dvurechenskii. FTP, **52**, 1346 (2018). (in Russian).

[16] Zh.V. Smagina, V.A. Zinovyev, G.K. Krivyakin, E.E. Rodyakina, P.A. Kuchinskaya, B.I. Fomin, A.N. Yablonskiy, M.V. Stepikhova, A.V. Novikov, A.V. Dvurechenskii. FTP, **52**, 1028 (2018). (in Russian).

[17] L.K. Orlov, V.I. Vdovin, N.L. Ivina, E.A. Steinman, Yu.N. Drozdov, M.L. Orlov. Crystals, **10**, 491 (2020).

[18] J. Greil, E. Bertagnolli, B. Salem, T. Baron, P. Gentile, A. Lugstein. Appl. Phys. Lett., **111**, 33103 (2017).

[19] M.L. Orlov, Yu.A. Romanov, L.K. Orlov. Microelectronics J., **36**, 396 (2005).

[20] M.L. Orlov, Yu.A. Romanov, L.K. Orlov. Proceed. SEMI-NANO2005, Budapest, Hungary, **2**, 325 (2005).

[21] L.K. Orlov, Yu.A. Romanov. Izv. vuzov. Radiofizika, **32**, 282 (1989). (in Russian).

[22] Yu.Yu. Romanova, M.L. Orlov, Yu.A. Romanov. FTP, **46**, 1475 (2012). (in Russian).

Translated by A.Akhtyamov